for subsequent studies. Experiments were conducted in accordance with protocols approved by the Harvard Medical School Animal Care Committee.

22. P. Pasinelli, D. R. Borchelt, M. K. Houseweart, D. W. Cleveland, R. H. Brown Jr., *Proc. Natl. Acad. Sci. U.S.A.* **95**, 15763 (1998).
23. To investigate whether caspase-1 and caspase-3 are activated in the mSOD1 mouse spinal cord, we performed immunohistochemical staining with an antibody specific for activated caspase-1 (provided by J. Yuan, Harvard Medical School, Boston, MA) and an antibody specific to activated caspase-3, which is also known as CM1 (provided by A. Srinivasan, Idun Pharmaceutical, La Jolla, CA). In addition, a neuron-specific marker, anti-NeuN antibody (Chemicon, Temecula, CA), was used in a double staining procedure to identify neuronal cells. At 70, 90, and 110 days of age, mice were killed and perfused with 4% paraformaldehyde. Spinal cords were removed under a dissecting microscope. Tissue was frozen in cold isopentane after cryoprotection in 30% sucrose. Frozen sections (10 μm thick) were washed with phosphate-buffered saline (PBS) containing 0.05% Tween-20 and were incubated with 5% normal goat serum. The sections were incubated overnight with rat polyclonal antibody to caspase-1 (1:5) or rabbit polyclonal antibody to caspase-3 (CM1) (1:2000), washed overnight, then washed three times with PBS, and finally probed with a biotinylated secondary antibody to rat immunogloblin G (IgG) or a biotinylated secondary antibody to rabbit IgG (1:300; Vector, Burlingame, CA) for 2 hours. Next, specimens were incubated in Fluorescein Avidin DCS (1:1000; Vector). Sections were also double stained with the NeuN antibody (1:100) followed by Texas Red antibody to mouse (1:200; Vector). Hoechst 33342 was used for counterstaining. The fluorescent stained sections were evaluated with epifluorescence microscopy.
24. At 60 days of age, osmotic pumps (Alzet, Palo Alto, CA) were used for the intracerebroventricular delivery of zVAD-fmk (Enzyme Systems, Livermore, CA). Pumps were filled with vehicle (0.4% dimethyl sulfoxide, 0.1 M Pipes, pH 6.9), 100 μg of 2 VAG-fmk per 20g body weight, or 300 μg of zVAG-fmk per 20 g of body weight. Pumps continuously delivered the drug for 28 days and were then exchanged for new pumps filled with fresh drug or vehicle for an additional 28-day treatment. The investigator was blind to the identity of the drug or vehicle used in the pump until the death of all mice.
25. A Rotarod (Columbus Instruments, Columbus, OH) was used to evaluate motor function. Mice were first evaluated the day before placement of the osmotic pumps and thereafter on a weekly basis. Mice were placed on the rotating rod at speeds of 5, 15, and 20 rpm. The time each mouse remained on the rod was registered automatically. If the mouse remained on the rod for 7 min, the test was completed and scored as 7 min.
26. Spinal cord and phrenic nerve samples were collected and processed as described (*10*). Motor neurons were counted on cryostat-cut sections (40 μm thick) stained with thionin. Quantification was performed by stereology as described by Liberatore *et al.* [*Nature Med.* **5**, 1403 1999] on every 10th spinal cord section, spanning the entire cervical and lumbar enlargements.
27. K. Kuida *et al.*, *Science* **267**, 2000 (1995).
28. Mature IL-1β concentration was measured with an enzyme-linked immunosorbent assay (ELISA) kit (R&D, Minneapolis, MN), which is specific for the mature form of the cytokine. Full-length spinal cord tissue was removed from mice treated with zVAD-fmk or vehicle at 100 days of age. Tissue was processed as previously described (*20*). Human spinal cord samples were generously provided by the Harvard, Massachusetts General Hospital, and Columbia brain banks.
29. R. M. Friedlander and J. Yuan, *Cell Death Differ.* **5**, 823 (1998).
30. R. M. Friedlander, V. Gagliardini, R. J. Rotello, J. Yuan, *J. Exp. Med.* **184**, 717 (1996).
31. Spinal cord tissue was obtained from 70-, 90-, and 110-day-old mice. Total RNA was extracted with Trizol (Life Technologies, Rockville, MD), and 1 mg was used as a template for first-strand synthesis. Primers were designed from published sequences (Life Technologies). Primers used to amplify caspase-1 were 5′-TGG TCT TGT GAC TTG GAG GA-3′ and 5′-TGG CTT CTT ATT GGC ACG AT-3′, resulting in a 191–base pair (bp) amplified product. For caspase-3, primer sequences were 5′-TGT CAT CTC GCT CTG GTA CG-3′ and 5′-AAA TGA CCC CTT CAT CAC CA-3′, resulting in a 200-bp amplified product. To confirm cDNA integrity and to standardize expression levels, we amplified fragments of glyceraldehyde phoshpate-3-dehydrogenase (GADPH)in parallel. Products were analyzed by electrophoresis in a 1.5% agarose gel and were visualized by ethidium bromide staining. A Chemi Doc imaging system (BioRad) was used for signal quantification. Signals are expressed as the ratio of band densities (caspase/GAPDH) of caspase expression in ALS and wild-type mice.
32. S. Holmin and T. Mathiesen, *J. Neurosurg.* **92**, 108 (2000).
33. J. Y. Yuan and H. R. Horvitz, *Dev. Biol.* **138**, 33 (1990).
34. M. Enari, R. V. Talanian, W. W. Wong, S. Nagata, *Nature* **380**, 723 (1996).
35. A. Ali *et al.*, *J. Hematother. Stem Cell Res.* **8**, 343 (1999).
36. M. Tewari *et al.*, *Cell* **81**, 801 (1995).
37. We thank A. Srinivasan for providing the CM1 antibody and J. Yuan for providing the caspase-1 antibody; M. Schoenebeck for expert preparation of the phrenic nerve samples; J. Yuan for insightful comments on the manuscript; and E. Friedlander for editorial assistance. Supported by the Muscular Dystrophy Association; the ALS Association; Project-ALS; the National Institute of Neurological Disorders and Stroke (grants R01 NS38586, R29 NS37345, and P50 NS38370); the U.S. Department of Defense (grant DAMD 17-99-1-9471); the Lowenstein Foundation; the Smart Foundation; and the Parkinson's Disease Foundation. C.G. is the recipient of a scholarship from the French ISERM. S.P. is a recipient of the Cotzias Award from the American Parkinson Disease Association.

4 February 2000; accepted 15 March 2000

The Outcome of Acute Hepatitis C Predicted by the Evolution of the Viral Quasispecies

Patrizia Farci,[1,2]* Atsushi Shimoda,[3] Alessandra Coiana,[1] Giacomo Diaz,[4] Giovanna Peddis,[1] Jacqueline C. Melpolder,[5] Antonello Strazzera,[1] David Y. Chien,[6] Santiago J. Munoz,[7] Angelo Balestrieri,[1] Robert H. Purcell,[2] Harvey J. Alter[5]

The mechanisms by which hepatitis C virus (HCV) induces chronic infection in the vast majority of infected individuals are unknown. Sequences within the HCV *E1* and *E2* envelope genes were analyzed during the acute phase of hepatitis C in 12 patients with different clinical outcomes. Acute resolving hepatitis was associated with relative evolutionary stasis of the heterogeneous viral population (quasispecies), whereas progressing hepatitis correlated with genetic evolution of HCV. Consistent with the hypothesis of selective pressure by the host immune system, the sequence changes occurred almost exclusively within the hypervariable region 1 of the *E2* gene and were temporally correlated with antibody seroconversion. These data indicate that the evolutionary dynamics of the HCV quasispecies during the acute phase of hepatitis C predict whether the infection will resolve or become chronic.

HCV infection is an important public health problem worldwide (*1*) because it is a major cause of chronic hepatitis, cirrhosis, and hepatocellular carcinoma (*2*). Very rarely, HCV causes fulminant hepatitis (FH), the most severe form of acute hepatitis. Although the infection resolves in 15% of cases, it becomes chronic in up to 85% of infected individuals (*3*). The clinical course of chronic hepatitis C is highly variable. In about 70% of the patients the disease is mild and stable over several decades, whereas in the remaining 30% it is more rapidly progressive. Prospective studies of hepatitis C have failed to identify any clinical, serologic, or virologic features that predict the outcome of the disease (*4*).

The mechanisms responsible for the high rate of viral persistence and for the variable clinical course of hepatitis C are unknown, but are thought to represent a complex interplay between viral diversity and host immunity (*5*). Although HCV infection induces strong cellular and humoral immune responses (*6, 7*), they are generally insufficient to

[1]Department of Medical Sciences, University of Cagliari, Via San Giorgio 12, 09124 Cagliari, Italy. [2]Hepatitis Viruses Section, Laboratory of Infectious Diseases, National Institute of Allergy and Infectious Diseases, National Institutes of Health (NIH), Bethesda, MD 20892, USA. [3]Department of Internal Medicine, Kanazawa University, Kanazawa 920-8641, Japan. [4]Department of Cytomorphology, University of Cagliari, 09124 Cagliari, Italy. [5]Department of Transfusion Medicine, Warren G. Magnuson Clinical Center, NIH, Bethesda, MD 20892, USA. [6]Chiron Corporation, Emeryville, CA 94507, USA. [7]Albert Einstein Medical Center, Philadelphia, PA 19141, USA.

*To whom correspondence should be addressed. E-mail: farcip@pacs.unica.it-

eradicate the virus or to prevent reinfection (*8, 9*). Over the past few years, evidence has accumulated to suggest that the genetic variation of HCV within the same individual—specifically, the simultaneous presence of different but closely related viral variants that are commonly defined as quasispecies (*10*)—may allow the virus to circumvent the immune response, leading to chronic infection. There is very limited information on the early evolution of the viral quasispecies during the acute phase of hepatitis C in patients who have been followed for a sufficient time to determine their long-term clinical outcome (*11*). Access to a well-defined cohort of prospectively studied patients enrolled in a study of post-transfusion non-A, non-B hepatitis gave us an opportunity to investigate the relationship between the genetic evolution of HCV early in the course of infection and the outcome of the disease.

We studied the number of viral variants, the genetic distance between the different variants (genetic diversity), and the evolution of HCV quasispecies, in parallel with the level of viral replication and the humoral immune response, during the incubation period and the acute phase of hepatitis C. Serial serum samples were obtained from 12 patients with hepatitis C (*12*) who were selected on the basis of their clinical outcome determined during prospective evaluation ranging up to 20 years (Table 1). Three patients had FH; three had acute, self-limited hepatitis characterized by clearance of serum HCV RNA within 16 weeks after transfusion; and six had acute hepatitis that progressed to chronicity, associated with persistent viremia. Among the latter six patients, the disease was mild and stable for more than 20 years in three (slow progressors), whereas in the remaining three it was severe and rapidly progressive, leading to liver-related death within 5 years of the onset of infection (rapid progressors) (Table 1).

The number of viral variants and the genetic diversity of the HCV quasispecies were assessed by examining viral sequences spanning the envelope genes (*E1* and *E2*) both within and outside the hypervariable region 1 (HVR1) (*13*). For all patients with resolving and progressing hepatitis, we studied the first available polymerase chain reaction (PCR)–positive sample (within 2 to 5 weeks of transfusion, mean 3.1 ± 1.2 weeks), one sample before antibody seroconversion [either before or at the time of the alanine aminotransferase (ALT) peak], and one or two samples after antibody seroconversion. For patients with FH, two samples were available for the analysis, one before and one after antibody seroconversion, with the exception of patient 3 (Table 1) (*12*). DNA amplified by PCR from the *E1/E2* genes (*14, 15*) was cloned and a mean of 10.6 molecular clones from each sample were sequenced (*16*) for a total of 414 sequences, each 558 nucleotides in length. Genetic diversity was calculated by analysis of the amino acid sequences using the mean Hamming distance (*17*). To determine the course of HCV viremia, we detected serum HCV RNA by a nested PCR assay (*18*) and quantified it with the branched-chain DNA test (*19*); we determined the HCV genotype by sequence analysis of part of the *E1* gene (*20*). All sera were tested for antibodies to structural and nonstructural proteins of HCV (*21*).

The genetic diversity and the number of viral variants within the HCV quasispecies, both in the first available PCR-positive sample and in the pre–antibody seroconversion sample, did not differ significantly between patients who resolved their infection and those who developed chronic disease (Fig. 1, A and B). In contrast, after antibody seroconversion, patients with resolving hepatitis showed a decrease in the genetic diversity of HVR1, whereas those with progressing hepatitis showed a marked increase in diversity (Fig. 1A). These different patterns are further illustrated by two representative cases shown in Fig. 2. When we compared the changes in genetic diversity between the last sample just before antibody appears and the first sample after antibody seroconversion, the difference in genetic diversity between resolving and progressing hepatitis was statistically significant (Table 2). Patients with FH, despite high serum levels of HCV RNA, showed the lowest degree of genetic diversity, both before and after antibody seroconversion (Fig. 1A). When we analyzed the genetic diversity in the *E1/E2* region outside HVR1, based on the analysis of 155 predicted amino acids, the viral diversity was consistently lower than within HVR1 and did not change over time in all patients examined, although patients with FH showed a trend toward an increase after seroconversion (Fig. 1A). Therefore, the different patterns observed in patients with resolving and progressing hepatitis were essentially due to genetic variation within HVR1. These data strongly suggest that this region is under selective pressure by the host immune system.

In contrast to the genetic diversity, the number of viral variants as assessed by HVR1 sequences did not show any specific correlation with disease outcome, although a slight increase was detected in patients who developed chronic hepatitis (Fig. 1B). Similar to the genetic diversity, the number of variants outside HVR1 was consistently lower than that within HVR1 in all patient groups throughout the course of the disease.

Table 1. Clinical and serologic evaluation of hepatitis C in prospectively followed patients. All numbers in parentheses indicate the week after transfusion. The level of viremia was measured by branched-chain DNA test (*19*). Antibodies to HCV and to E2 protein were measured as described (*21*). ND, not determined; NA, not applicable, because the risk factor was unknown and therefore the time of infection could not be ascertained.

Disease outcome and patient number	Liver-related death	Viral genotype	Age	Sex	Blood units (no.)	Peak serum ALT (IU/liter)	Viremia: Peak serum HCV RNA (equiv/ml)	Anti-HCV	Anti-E2
Fulminant									
1	Yes	1b	68	M	130	4493 (5)	1.6×10^8 (5)	+ (6)	ND
2	Yes*	1a	35	F	4	392 (12)	2.6×10^8 (10)	+ (8)	ND
3	Yes	2a	67	F	NA	2160 (NA)	$<3.5 \times 10^5$ (NA)	+ (NA)	ND
Resolving									
4	No	1a	71	M	35	1332 (12)	2.6×10^7 (12)	+ (12)	+ (13)
5	No	1a	25	F	4	915 (8)	2.9×10^7 (5)	+ (10)	+ (5)
6	No	1b	65	F	34	1244 (6)	6.1×10^7 (5)	+ (5)	+ (9)
Slow progressor									
7	No	1b	57	F	13	522 (8)	4.4×10^5 (6)	+ (9)	+ (4)
8	No	1b	55	M	14	775 (12)	6.1×10^6 (10)	+ (11)	+ (5)
9	No	1a	60	M	19	2112 (8)	2.2×10^8 (7)	+ (8)	+ (9)
Rapid progressor									
10	No†	1a	59	M	7	755 (17)	5.6×10^8 (13)	+ (10)	+ (5)
11	Yes	1a	62	M	15	1300 (18)	4.6×10^5 (16)	+ (12)	+ (9)
12	Yes	1b	63	F	8	1200 (10)	6.6×10^6 (13)	+ (15)	+ (9)

*After orthotopic liver transplantation (OLT), the patient developed fulminant hepatitis C (*12*), for which she received a second OLT; she died several weeks after the second OLT. †The patient died of complications of heart disease and diabetes, but also had an active cirrhosis and a small hepatocellular carcinoma that was found at autopsy.

To investigate whether the different patterns of viral genetic variation were due to positive selection, we measured the number of synonymous (silent) nucleotide substitutions per synonymous site and the number of nonsynonymous (amino acid replacement) nucleotide substitutions per nonsynonymous site (*22*), both within and outside HVR1; sequences obtained from each time point were compared with the consensus (reference) sequence of the first time point. This analysis revealed a difference in virus evolution according to the outcome of the disease. Comparison of genetic distances between the earliest and the latest sample from each patient revealed that the mean number of nonsynonymous substitutions per site per week within HVR1 was significantly higher in progressing hepatitis [mean ± SEM, 7.0 (±1.7) × 10^{-3}] than in resolving [2.0 (±0.9) × 10^{-3}; $P = 0.037$] or fulminant [0.4 (±0.4) × 10^{-3}; $P = 0.011$] hepatitis, whereas outside HVR1 it was consistently lower in all groups and did not differ significantly among progressing [1.1 (±0.3) × 10^{-3}], resolving [0.3 (±0.1) × 10^{-3}], and fulminant [0.5 (±0.03) × 10^{-3}] hepatitis. By contrast, the mean number of synonymous substitutions within HVR1 was comparable among the three groups, although it was slightly higher in fulminant [4.9 (±3.9) × 10^{-3}] than in progressing [4.1 (±1.1) × 10^{-3}] and resolving [3.6 (±2.6) × 10^{-3}] hepatitis; similarly, outside HVR1, it was higher in fulminant [4.1 (±2.6) × 10^{-3}] than in progressing [2.1 (±0.6) × 10^{-3}] and resolving [1.5 (±1.0) × 10^{-3}] hepatitis. Thus, in FH there was a striking amino acid conservation both within and outside HVR1, despite a high rate of viral replication and synonymous substitutions.

Phylogenetic analysis of all the HVR1 amino acid sequences obtained from each patient at different time points showed two topological patterns according to the outcome of the disease. In resolving hepatitis, there was generally a monophyletic population with intermingling of sequences derived from different time points (Fig. 3A). In progressing hepatitis, there was a tendency to form clusters over time (Fig. 3B) and the branch lengths were consistently longer than those seen in acute resolving hepatitis (*23*). By contrast, when HVR1 was excluded, the phylogenetic reconstructions of the rest of the *E1/E2* region showed a monophyletic population in each patient, with very short branch lengths, and no difference between resolving and progressing hepatitis (*24*). The greater genetic distances seen in patients with progressing hepatitis correlated with a higher accumulation rate of nonsynonymous substitutions, consistent with a positive selection for change within HVR1.

We next determined whether the pattern of evolution of the viral quasispecies in progressing hepatitis differed between slow and rapid progressors. Although there was a distinct difference in the rate and extent of viral evolution between patients who resolved their infection and those who progressed to chronicity, the distinction between slow and rapid progressors during the first 4 months of infection was equivocal. We also examined whether the pattern of genetic evolution observed in progressing hepatitis correlated with specific clinical, virological, or immunological parameters. Our study showed that the degree of genetic heterogeneity did not correlate with either the number of units of blood received or the number of donors. Similarly, the genetic diversity and the number of viral variants did not correlate with the level of viremia. Also, no significant association was found between the serum level of HCV RNA or the HCV genotype and the outcome of the disease.

Our study provides evidence that the outcome of acute hepatitis C may be determined in the early phase of primary infection. Acute hepatitis that progressed to chronicity correlated with genetic evolution of HCV within the first 4 months of infection. In agreement with the paradigm proposed for HIV infection (*25, 26*), the presence of diverse viral forms may reflect shifts in the virus population possibly related to changes in the host environment, such as the appearance of neutralizing antibodies or intra-

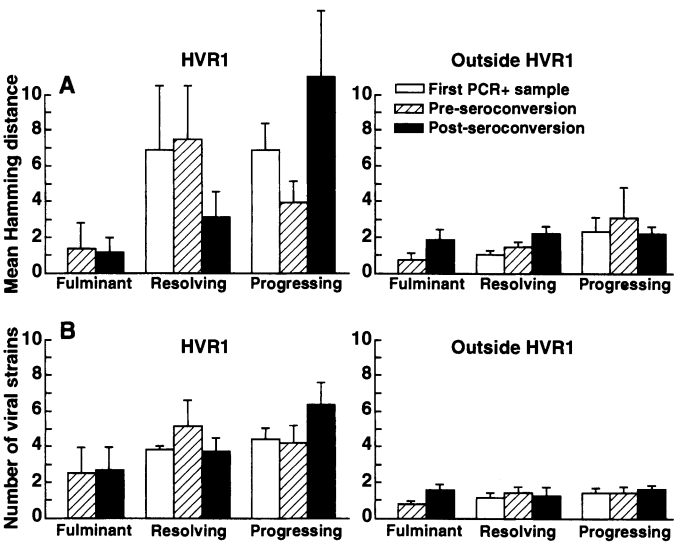

Fig. 1. Genetic distance among the variants (diversity) and number of viral strains of the HCV quasispecies within and outside HVR1 in fulminant, resolving, and progressing hepatitis. (**A**) Genetic diversity within the viral quasispecies, as measured by mean Hamming distance (*17*). (**B**) Number of different viral strains detected in the viral quasispecies. The values indicate the number of variants per 31 amino acids both within and outside HVR1. The data represent the mean (±SEM) of the results obtained from all the patients within each group at different time points. In fulminant hepatitis the analysis before antibody seroconversion was extended to only two patients, because only a single sample was available from patient 3 [Table 1 (*12*)].

Table 2. Comparison of changes in genetic diversity and in number of viral strains in fulminant, resolving, and progressing hepatitis.

Patient group	No. of patients	Time points†	Interval (weeks)	Change in genetic diversity*		Change in number of viral strains	
				HVR1	*E1/E2* outside HVR1	HVR1	*E1/E2* outside HVR1
Fulminant hepatitis	2‡	b vs. c	1.7 ± 0.3	−0.03 ± 0.03	0.7 ± 0.8	0.5 ± 0.5	3.0 ± 3.0
Resolving hepatitis	3	a vs. b	4.5 ± 1.5	1.0 ± 3.0	0.5 ± 0.05	2.0 ± 2.0	1.5 ± 0.5
		a vs. c	7.5 ± 2.5	−3.7 ± 2.6	0.2 ± 0.2	0.0 ± 0.6	0.3 ± 2.2
		b vs. c	3.0 ± 0.5	−4.4 ± 1.7§	−0.1 ± 0.4	−1.3 ± 0.9	−0.7 ± 2.3
Progressing hepatitis	6	a vs. b	5.6 ± 1.3	−2.9 ± 1.7	0.8 ± 1.6	0.2 ± 0.5	0.0 ± 1.3
		a vs. c	11.0 ± 1.3	4.1 ± 2.7	−0.2 ± 0.6	1.7 ± 1.4	0.8 ± 0.8
		b vs. c	5.3 ± 1.5	7.0 ± 3.4§	−1.0 ± 1.5	1.8 ± 1.4	0.8 ± 0.9

*Genetic diversity was assessed by mean Hamming distance (*17*). The data represent means ± SEM. Negative values indicate a reduction in genetic diversity and in number of viral strains; positive values indicate an increase in genetic diversity and in number of viral strains. †The first time point (a) corresponds to the baseline, the second (b) before antibody seroconversion, and the third (c) after antibody seroconversion. ‡Two patients with fulminant hepatitis C were analyzed. §$P = 0.020$ for the comparison of time points b versus c of resolving versus progressing hepatitis, by unpaired Welch's t test (*31*).

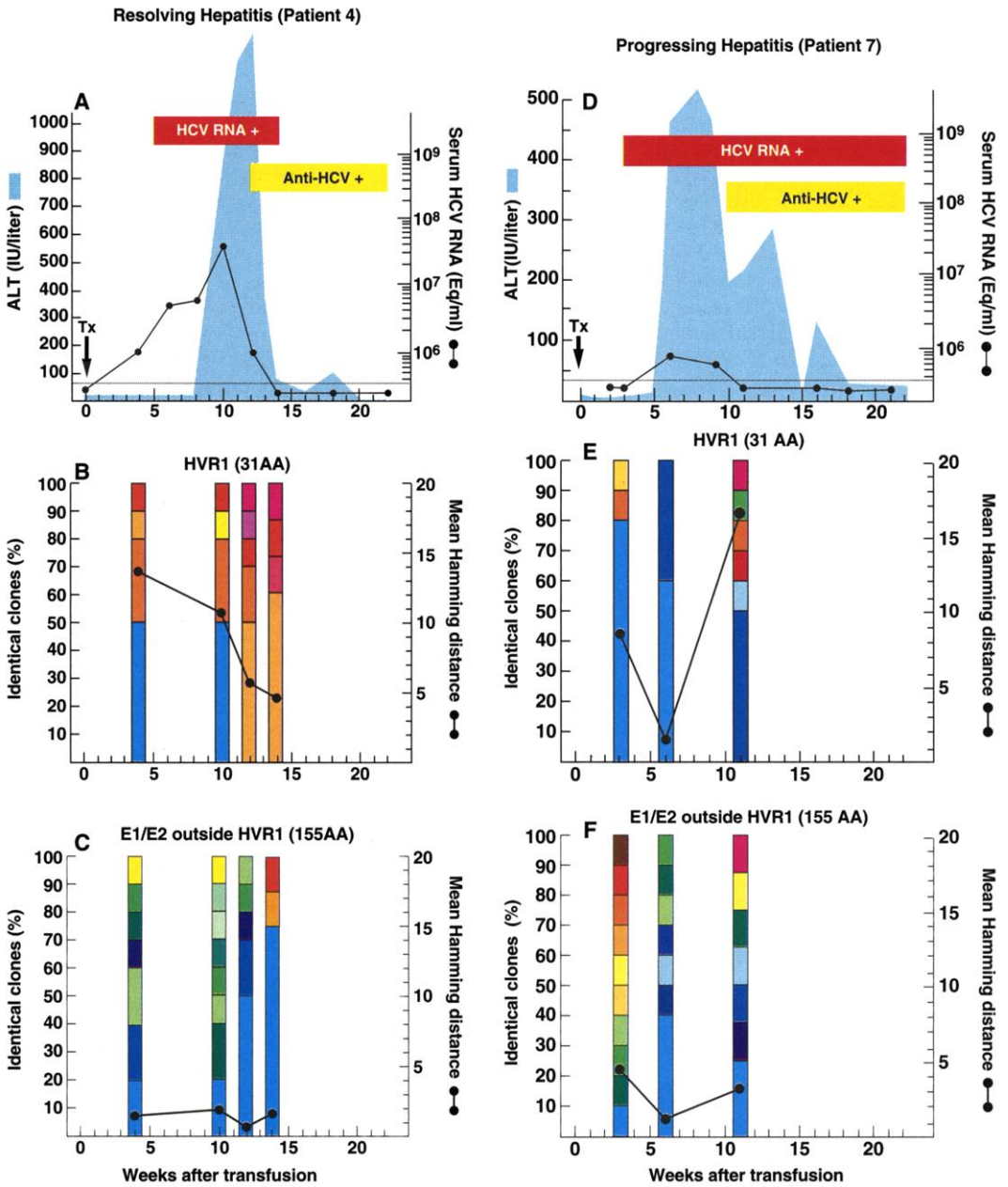

Fig. 2. Evolution of HCV quasispecies during the course of acute hepatitis C in two representative patients, one with resolving hepatitis and one with acute hepatitis that progressed to chronicity with a stable course. Patient numbers are the same as in Table 1. (**A** and **D**) Clinical course of hepatitis C. The gray areas indicate ALT levels. The red horizontal bars indicate positive assays for serum HCV RNA by PCR. The black lines indicate the titer of serum HCV RNA by the branched-chain DNA assay, on a logarithmic scale. The yellow horizontal bars indicate antibodies to HCV detected by second-generation assays. Tx denotes the time of blood transfusion. (**B** and **E**) Number of viral variants and diversity (genetic distance among variants) of the HCV quasispecies within the 31 amino acids of HVR1. The vertical bars indicate the number and the proportion of viral variants within each sample. Within the vertical bars, each variant is identified by a different color. The dominant viral variant found in each patient at the first time point is indicated in turquoise; other variants are indicated by additional colors. The same color indicates identity between viral variants detected at different time points within each patient, but not between different patients. The viral population diversity (black line) was calculated by mean Hamming distance from the predicted amino acid sequences obtained from each sample (*17*). (**C** and **F**) Number of viral variants and genetic diversity of HCV within 155 amino acids from the *E1/E2* region, spanning map positions 318 to 503, with the exclusion of the 31 amino acids of HVR1. [For a similar analysis of two other cases, representing fulminant hepatitis and chronic hepatitis with a rapidly progressive course, see *Science* Online (www.sciencemag.org/feature/data/1047689.shl).]

hepatic cytotoxic T lymphocytes. Under these selective constraints, viral population disequilibrium may emerge with the selection of variant viruses with enhanced ability to persist in the host (*27*). The evidence in our patients of a temporal association between viral evolution and the first emergence of a specific immune response corroborates this hypothesis. Moreover, because the amino acid substitutions occurred almost exclusively within HVR1, a critical target of selective pressure by the immune system (*5, 28*), this domain may play a role in the pathogenesis of HCV infection and, in particular, in the progression to chronicity.

Although our findings on progressing hepatitis C suggest that there was no predominant viral form with enhanced pathogenic potential, FH was characterized by a homogeneous viral population. These data suggest that in fulminant hepatitis C there is a trend to preserve the unique fitness of a particular viral variant, which supports the hypothesis that the inherent virulence of a specific HCV strain may lead to massive hepatocellular necrosis.

Spontaneous viral clearance occurs in about 15% of patients after primary HCV infection (*3*). Although the immunological correlates of HCV clearance are still undefined, the earliest events in the virus-host interaction are likely to determine the outcome of infection. In this context, the observation that viral clearance correlates with a reduction in viral diversity over time may appear counterintuitive, as it might suggest the absence of effective immune responses exerting a selective pressure for change. The alternative and, we feel, more likely hypothesis is that the specific humoral or cellular immune responses against HCV are more effective in patients who resolve their infection, as suggested by recent studies (*29*), and that the genetic diversity of HCV quasispecies declines as a result of the progressive clearance of individual variants. Thus, when the immune response against HCV is optimal, viral variation is eventually contained and the strains become increasingly homogeneous until the final variant is effectively cleared. A similar trend, with a significant decrease in genetic diversity and in the number of HCV variants, has been documented in patients with a favorable response to interferon therapy during the first 2 weeks of treatment

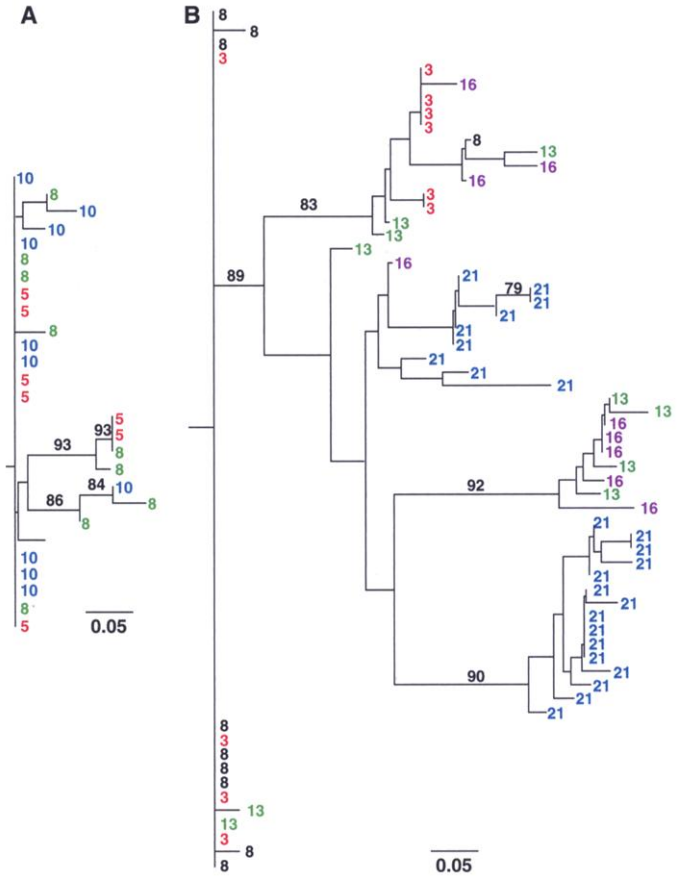

Fig. 3. Representative phylogenetic reconstructions showing the evolutionary relationships of all viral amino acid sequences of HVR1, within patients. The phylogenetic trees were constructed with the neighbor-joining method, using the NEIGHBOR program in the PHYLIP package (*32*). Genetic distances were calculated with PROTDIST from the PHYLIP package based on Kimura's distance. A bootstrap analysis using 100 bootstrap replicates was performed to assess the reliability at each of the internal nodes of the trees. The numbers at branch points indicate the percentage of the bootstrap resamplings; frequencies greater than 75% are shown. Substantially similar trees were generated using the Fitch-Margoliash distance method using the Fitch program available from the PHYLIP package. Clones are shown by a number indicating weeks from the time of primary infection, with each time point represented by a different color. The scale bar below each tree indicates the genetic distance based on Kimvra's formula. (**A**) The viral sequences were selected to represent the pattern seen in patients with acute resolving hepatitis. The phylogenetic reconstruction showed a monophyletic viral population with intermingling of sequences from different time points. (**B**) The viral sequences were selected to represent the pattern seen in patients who developed progressing hepatitis. The phylogenetic reconstruction showed sequential shifts in the viral population after 8 weeks from the time of infection. Some intermingling of sequences from sequential time points was also observed.

(*30*). Our findings have prognostic implications, because an increase in HVR1 diversity during acute infection predicts progression to chronic disease, whereas a decrease correlates with resolution of the disease. The direct implication of HVR1, the most variable region of HCV, in the development of chronic HCV infection poses a major challenge for devising preventive and therapeutic strategies against HCV.

References and Notes

1. National Institutes of Health Consensus Development Conference Panel, *Hepatology* **26** (suppl. 1), 2S (1997).
2. K. Nishioka *et al.*, *Cancer* **67**, 429 (1991); L. B. Seeff, *Hepatology* **26** (suppl. 1), 21S (1997); A. M. Di Bisceglie *et al.*, *Hepatology* **14**, 969 (1991).
3. H. J. Alter and L. B. Seeff, in *Viral Hepatitis*, A. Z. Zuckerman and H. C. Thomas, Eds. (Churchill Livingstone, Edinburgh, UK, 1997), pp. 467–498.
4. J. H. Hoofnagle, *Hepatology* **26** (suppl. 1), 15S (1997); L. B. Seeff *et al.*, *N. Engl. J. Med.* **327**, 1906 (1992); M. J. Tong, N. S. el-Farra, A. R. Reikes, R. L. Co, *N. Engl. J. Med.* **332**, 1463 (1995).
5. A. J. Weiner *et al.*, *Proc. Natl. Acad. Sci. U.S.A.* **89**, 3468 (1992); S. Taniguchi *et al.*, *Virology* **195**, 297 (1993); N. Kato *et al.*, *J. Virol.* **67**, 3923 (1993).
6. H. J. Alter, *Blood* **85**, 1681 (1995).
7. C. Ferrari *et al.*, *Hepatology* **19**, 286 (1994); F. V. Chisari, in *Viral Hepatitis and Liver Diseases*, M. Rizzetto, R. H. Purcell, J. L. Gerin, G. Verme, Eds. (Minerva Medica, Torino, Italy, 1997), pp. 405–415.
8. P. Farci *et al.*, *Science* **258**, 135 (1992).
9. A. M. Prince *et al.*, *J. Infect. Dis.* **165**, 438 (1992); M. E. Lai *et al.*, *Lancet* **343**, 388 (1994).
10. M. Martell *et al.*, *J. Virol.* **66**, 3225 (1992).
11. A. Manzin *et al.*, *J. Virol.* **72**, 6271 (1998); S. C. Ray *et al.*, *J. Virol.* **73**, 2938 (1999).
12. A total of 12 patients were included in this study. Ten patients, four women and six men (mean age ± SD, 58.5 ± 12.74 years), were derived from a prospective study of post-transfusion non-A, non-B hepatitis conducted at NIH [D. E. Koziol *et al.*, *Ann. Intern. Med.* **104**, 488 (1986)]. One patient had FH, three had acute self-limited hepatitis, and six had acute hepatitis that progressed to chronicity. The remaining two patients with FH were derived from a study on the prevalence of HCV in non-A, non-B FH conducted at Jefferson Hospital, Philadelphia (S. J. Munoz, unpublished data). Both patients were females, mean age 51.0 ± 22.6 years. For patient 2 the risk factor for HCV infection was transfusion of red blood cells; there were no known risk factors for patient 3 (Table 1). Patient 2 was referred for liver transplantation for cryptogenic end-stage liver cirrhosis. Because of her chronic anemia, she was transfused before the first liver transplantation, prior to the introduction of universal anti-HCV screening. The patient seroconverted about 10 days after the first liver transplantation and 6 weeks later developed fulminant hepatic failure for which she received the second liver transplantation, but several weeks later died in hepatic coma [P. Farci *et al.*, *J. Infect. Dis.* **179**, 1007 (1999)]. Serial serum samples were available from all 12 patients, except patient 3, for whom only a single sample was available. This patient died of fulminant hepatic failure a few days after admission to the hospital.
13. A. J. Weiner *et al.*, *Virology* **180**, 842 (1991); M. Hijikata *et al.*, *Biochem. Biophys. Res. Commun.* **175**, 220 (1991).
14. P. Farci *et al.*, *N. Engl. J. Med.* **325**, 98 (1991).
15. Total RNA extracted from 100 μl of serum or plasma with TRIzol reagent (Gibco BRL) was reverse-transcribed in a volume of 20 μl, and the resulting cDNA was amplified using one set of primers from the *E1* and *E2* genes of the HCV genome, including HVR1 (*8*). The sensitivity, specificity, and details of our nested PCR technique have been reported (*8, 14*). We took precautions to reduce the risk of contamination [S. Kwok and R. Higuch, *Nature* **339**, 237 (1989)]. In addition, for each test sample, we included and tested a negative control in parallel throughout the entire procedure.
16. The PCR products amplified from the *E1/E2* region of the HCV genome were purified by Geneclean (BIO 101, La Jolla, CA), cloned into pGEM-T vector systems (Promega), and transformed into *Escherichia coli* strain J109. Plasmid DNA was extracted with the Qiagen plasmid kit and sequenced using the Applied Biosystems model 373 automated DNA sequencer with a modified Sanger method. For more technical information about quantification of the target DNA sequences, see *Science* Online (www.sciencemag.org/feature/data/1047689.shl).
17. The viral population diversity was calculated by analysis of predicted amino acid sequences, 186 amino acids in length, amplified from the *E1* and *E2* genes of the HCV genome, including the 31 amino acids of HVR1. The genetic diversity was calculated by the Hamming distance, which is defined as the number of amino acid differences between two sequences [R. W. Hamming, *Coding and Information Theory* (Prentice-Hall, Englewood Cliffs, NJ, ed. 2, 1986)]. The mean Hamming distance (that is, the average of the values taken for all sequence pairs derived from a single sample) was separately calculated on HVR1 (31 amino acids) and on the entire sequence outside HVR1 (155 amino acids). More details of this analysis are given in *Science* Online (www.sciencemag.org/feature/data/1047689.shl).
18. The nested primers derived from the 5′ noncoding region have been described (*8*).
19. Serum levels of HCV RNA were measured by the branched-chain DNA test with the Amplex Chiron Assay.
20. J. Bukh, R. H. Purcell, R. H. Miller, *Proc. Natl. Acad. Sci. U.S.A.* **90**, 8234 (1993).
21. Antibodies to HCV were tested weekly or biweekly by a second-generation enzyme immunoassay (EIA; Abbott Laboratories, North Chicago, IL). Antibodies to E2 protein were measured with an experimental EIA test. A full description of this assay is given in *Science* Online (www.sciencemag.org/feature/data/1047689.shl).
22. The average number of synonymous substitutions per synonymous site and the number of nonsynonymous substitutions per nonsynonymous site relative to the ancestral consensus sequence were calculated [M. Nei and T. Gojobori, *Mol. Biol. Evol.* **3**, 418 (1986)] for each time point within a single patient with the use of the program MEGA [S. Kumar, K. Tamura, M. Nei, *Molecular Evolutionary Genetics Analysis (MEGA)* version 1.01, Institute of Molecular Evolutionary Genetics, Pennsylvania State University]. The consensus sequence from the first time point was used as a reference. Comparison of the mean number (±SEM) of synonymous and nonsynonymous nucleotide substitutions per site per week between progressing and resolving or FH was performed by unpaired Welch's *t* test (*31*). In FH, the analysis was restricted to two patients, because only a single sample was available from patient 3 (*12*).
23. For each patient, we calculated the median branch lengths and the range from the ancestral node to all taxa from a single time point, based on Kimura's distance to generate a neighbor-joining tree. The time point after antibody seroconversion was used for this analysis. The median branch lengths and the range were as follows (patient numbers refer to Table 1): **patient 1,** week 7, 0.000 (0.000–0.000); **patient 2,** week 8, 0.000 (0.000–0.033); **patient 3,** 0.000 (0.000–0.034) [the

time of infection was unknown (Table 1) (*12*)]; **patient 4,** week 12, 0.017 (0.000–0.142); **patient 5,** week 10, 0.000 (0.000–0.106); **patient 6,** week 5, 0.000 (0.000–0.068); **patient 7,** week 11, 0.085 (0.033–0.318); **patient 8,** week 18, 0.422 (0.422–0.581); **patient 9,** week 9, 0.000 (0.000–0.308); **patient 10,** week 13, 0.265 (0.000–0.469); **patient 11,** week 16, 0.094 (0.000–0.094); **patient 12,** week 18, 0.033 (0.000–0.070). There was a trend toward an increase in the branch length from fulminant (patients 1 to 3) to acute resolving (patients 4 to 6) to progressing hepatitis (patients 7 to 12). One exception was represented by the median of patient 9, although the same case had a branch length maximum consistent with the trend observed in progressing hepatitis.

24. P. Farci *et al.*, data not shown.
25. S. M. Wolinsky *et al.*, *Science* **272**, 537 (1996).
26. M. Coffin, *Curr. Top. Microbiol. Immunol.* **176**, 181 (1992).
27. M. Eigen and C. K. Biebricker, in *RNA Genetics*, E. Domingo *et al.*, Eds. (CRC, Boca Raton, FL, 1988), vol. 3, pp. 211–245; D. A. Steinhauer and J. J. Holland, *Annu. Rev. Microbiol.* **41**, 409 (1987); J. J. Holland, J. C. La Torre, D. A. Steinhauer, *Curr. Top. Microbiol. Immunol.* **176**, 1 (1992); S. Wright, *Evolution and the Genetics of Populations* (Univ. of Chicago Press, Chicago, 1977), vols. 1 to 4; *Evolution* **36**, 427 (1982).
28. A. Zibert, E. Schreier, M. Roggendorf, *Virology* **208**, 653 (1995); P. Farci *et al.*, *Proc. Natl. Acad. Sci. U.S.A.* **93**, 15394 (1996); Y. K. Shimizu *et al.*, *Virology* **223**, 409 (1996); D. Rosa *et al.*, *Proc. Natl. Acad. Sci. U.S.A.* **93**, 1759 (1996); U. Kumar, J. Monjardino, H. C. Thomas, *Gastroenterology* **106**, 1072 (1994); M. U. Mondelli *et al.*, *Hepatology* **30**, 537 (1999).
29. H. M. Diepolder *et al.*, *Lancet* **346**, 1006 (1995); G. Missale *et al.*, *J. Clin. Invest.* **98**, 706 (1996); S. Cooper *et al.*, *Immunity* **10**, 439 (1999).
30. P. Farci *et al.*, *Proceedings of the 6th International Symposium on Hepatitis C and Related Viruses* (NIH, Bethesda, MD, 6–9 June 1999), p. 80.
31. B. L. Welch, *Biometrika* **29**, 350 (1938).
32. J. Felsenstein, *PHYLIP* version 3.573c (University of Washington, Seattle, 1993).

33. We thank E. Pascariello and A. Brambilla for their help in genetic analysis, P. Lusso for critical reading of the manuscript, and C. Bosoni and H. Newman for editorial assistance. Sequences have been submitted to GenBank under accession numbers AF245706 and AF246119.

6 December 1999; accepted 28 February 2000

Regulation of Area Identity in the Mammalian Neocortex by *Emx2* and *Pax6*

Kathie M. Bishop,[1] Guy Goudreau,[2] Dennis D. M. O'Leary[1]*

The contribution of extrinsic and genetic mechanisms in determining areas of the mammalian neocortex has been a contested issue. This study analyzes the roles of the regulatory genes *Emx2* and *Pax6*, which are expressed in opposing gradients in the neocortical ventricular zone, in specifying areas. Changes in the patterning of molecular markers and area-specific connections between the cortex and thalamus suggest that arealization of the neocortex is disproportionately altered in *Emx2* and *Pax6* mutant mice in opposing manners predicted from their countergradients of expression: rostral areas expand and caudal areas contract in *Emx2* mutants, whereas the opposite effect is seen in *Pax6* mutants. These findings suggest that *Emx2* and *Pax6* cooperate to regulate arealization of the neocortex and to confer area identity to cortical cells.

The mature mammalian neocortex is tangentially organized into distinct areas that serve specialized functions, such as sensory processing and motor control. These areas can be distinguished by differences in their input and output connections and architecture. It is assumed that the specification and differentiation of neocortical areas are controlled by an interplay between epigenetic (extrinsic) and genetic (intrinsic) mechanisms. Numerous studies suggest that diverse parts of the neocortex initially share potentials to develop features unique to a specific area (*1*) and have implicated thalamocortical input as a major epigenetic influence in this process (*2, 3*). Evidence for genetic regulation of arealization is limited to descriptions of graded or restricted patterns of gene expression in the embryonic neocortex (*4–6*) that are established independent of thalamocortical input (*5, 6*). Remaining unidentified, though, are genes that regulate arealization, presumably by conferring area identities to cortical cells and controlling the differential expression of downstream genes that govern, among other things, the area-specific targeting of thalamocortical afferents.

The regulatory genes that control neocortical arealization are assumed to be expressed in graded or restricted patterns in the embryonic cortex (*3*). Two genes that meet this criterion are the homeodomain transcription factor *Emx2* and the paired-box–containing transcription factor *Pax6*. Both genes are expressed in the dorsal telencephalic neuroepithelium, the proliferative zone that gives rise to cortical neurons (*7–9*). *Emx2* is expressed in low rostral to high caudal and low lateral to high medial gradients (*7, 8*), whereas *Pax6* is expressed in low caudal to high rostral and low medial to high lateral gradients (*8, 9*). On the basis of these expression patterns, we hypothesized that *Emx2* preferentially imparts caudal and medial area identities to cortical neurons, whereas *Pax6* preferentially imparts rostral and lateral identities (Fig. 1).

We have used molecular and connectional markers of area identity to test these hypotheses in mutant mice lacking either *Emx2* (*10*) or *Pax6* [*Small eye* (*Sey*)] (*11*) functional alleles. We predicted that, in the *Emx2* mutant neocortex, caudal and medial identities would be lost, resulting in a caudal and medial shift in rostral and lateral area identities (Fig. 1B). Conversely, we predicted that, in the *Pax6* mutant neocortex, rostral and lateral identities would be lost, resulting in a rostral and lateral shift in caudal and medial area identities (Fig. 1C). *Emx2* and *Pax6* (*Sey/Sey*) mutant mice die within hours after birth (*10, 11*), limiting our analysis to the late embryonic period, before the mice die but after some features of arealization have become evident.

The type II classical cadherins, *Cadherin6* (*Cad6*) and *Cadherin8* (*Cad8*), are expressed in areal patterns in the late embryonic mouse neocortex: *Cad8* has been reported to mark the rostrally located motor area, and *Cad6* marks the somatosensory area, located immediately caudal to the motor area, and the auditory area, located in the caudolateral neocortex (*12*). Because the cortex is reduced in size in both *Emx2* and *Pax6* mutants compared to wild type (Tables 1 through 5), we determined the proportion of the cortical surface covered by domains of cadherin expression as well as their absolute size (Fig. 2, B and D). No change in proportional sizes of cadherin expression domains would indicate that arealization per se has not been affected, suggesting that the full range of putative area identities is present in the smaller cortex and that all areas are uniformly reduced in size. A change in proportional sizes would indicate that areas are disproportionately affected in the mutant neocortex and therefore that *Emx2* and/or *Pax6* has a role in regulating arealization of the neocortex. This finding and interpretation would be most strongly supported by a change in absolute sizes of cadherin expression domains.

The areal pattern of cadherin expression in the *Emx2* homozygous mutant cortex (*13*) is substantially different than that in wild type (Fig. 2). The domain of *Cad8* expression is expanded caudally (Fig. 2A). This expansion appears to be greater along the medial edge of the cortex than farther laterally, suggesting that *Cad8* expression may also be expanded medially. The domain of *Cad6* expression is shifted caudally and medially, as seen on the dorsal and

[1]Molecular Neurobiology Laboratory, The Salk Institute for Biological Studies, 10010 North Torrey Pines Road, La Jolla, CA 92037, USA. [2]Max-Planck-Institute for Biophysical Chemistry, Department of Molecular Cell Biology, Am Fassberg 11, 37077 Göttingen, Germany.

*To whom correspondence should be addressed. E-mail: doleary@salk.edu